CFD Flow Analysis of the Influence of Rotor Seals in a Cantilever Microturbine

Tomáš Syka[1,*], *Andreas* P. Weiß[2], and *Richard* Matas[1]

[1]New Technologies - Research Centre (UWB), Univerzitní 2732/8, Pilsen, Czech Republic
[2]OTH Amberg-Weiden, Kaiser-Wilhelm-Ring 23, Amberg, Germany

Abstract. The article describes the results from the research and development of a cantilever microturbine designed for ORC power plants. The main objective of the paper was to compare different types of rotor seals and their effect on the turbine efficiency and rotor forces. The turbine stage and the numerical models used in the CFD system NUMECA FINE/Turbo are briefly described. The results are compared with the values obtained from measurements and previous simulations. The results show a relatively limited influence of the seal design on the turbine efficiency. The results also show the effect of the seal on the rotor axial force.

Keywords: *CFD simulation; NUMECA; ORC; leakages; rotor seal; cantilever micro-turbine*

1 Introduction

The number of decentralized small-scale stationary electrical energy sources (< 100 kW_{el}) connected to electricity distributing networks is growing and their development requires adjustments to the operation of these systems [1]. An example of such a source is the Organic Rankine Cycle (ORC) power plant, heated by e.g. waste heat from industry or from internal combustion engines, geothermal heat or even solar radiation.

An ORC power plant works like a coal-fired steam power plant but the difference between ORC and the conventional steam cycle is that instead of water, another fluid like alcohol, a refrigerant or siloxanes is used. More information about micro-turbines in general can be found in [2, 3]. This paper deals mainly with CFD simulations of geometric modifications of a small cantilever turbine with a radial inlet direction into the stator channels and a radial outlet from the rotor.

1.1 The turbine and the ORC test plant

The design of the cantilever microturbine is simple compared to a generic steam turbine and to keep costs low it is advisable to design a single stage turbine, despite its lower efficiency [4, 5, 6]. It is also possible to use multi-stage turbines but the efficiency benefits of this solution are not conclusive and it is more complex and therefore more expensive [7]. It is also necessary to develop a very flexible "construction kit" due to the wide range of

* Corresponding author: tsyka@ntc.zcu.cz

temperatures and pressures of the operating conditions depending on the specific heat source [8].

The turbine design, including the generator, is really compact and the dimensions of the whole unit are relatively small – see Fig. 1 left. The maximum diameter of the rotor wheel is 120 mm. The main parts of this unit are the inlet casing, stator wheel with nozzles, rotor wheel, outlet casing and generator. The concept, design and application of this turbine is proven and this work only focuses on its fine-tuning [4]. Another option is the ELEKTRA type re-entry turbine. This research is intensively underway. The ELEKTRA turbine has the advantage of a lower operational speed (leading to a cheaper electrical generator) and the aim is now to achieve an efficiency comparable to the "classic" turbine type presented in [9, 10].

In order to investigate real characteristics of the cantilever turbine, it was tested in the ORC research plant at the Centre for Energy Technology (ZET) at the University of Bayreuth. The research plant was designed to investigate the waste heat recovery from a 250kW biogas internal combustion engine with an exhaust gas temperature of about 500 °C – see Fig. 1 right. The microturbine works with hexamethyldisiloxane as a working fluid [11, 12, 13]. More information about the turbine and the ORC research plant layout and its parameters has been published in paper [14]. There are no seals to lower leakage losses in the basic design of the microturbine.

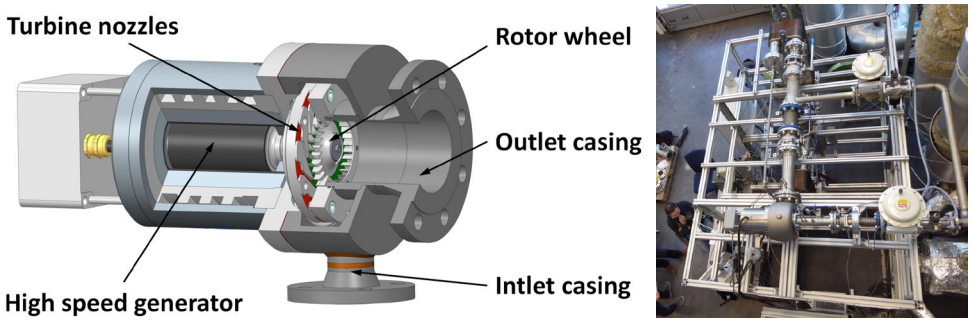

Fig. 1. Layout of the radial inflow cantilever turbine (left) and the ORC test rig (right) [14].

1.2 The CFD simulations and their goal

This work and the presented results are based on CFD simulations published in paper [14]. The work describes the comparison of measured and CFD results and an investigation of the influence of the outlet geometry on the turbine working parameters. As mentioned above, there are no seals in this basic turbine design. Therefore, the main objective of the follow-up work was to build on the simulations and to compare the different types of rotor seals and their possible influence on the turbine efficiency and the magnitude of the axial force acting on the rotor.

2 CFD setup and design of the rotor seal

CFD simulations of microturbines have specific features due to their functional principle. The working fluid enters the turbine with low velocity and high pressure values. The expansion to very low pressure occurs in the stator nozzles. This is associated with a high increase of the flow velocity. The flow velocity at the outlet of the stator nozzles is supersonic and the Mach number is usually higher than 2.5. The high Mach number and the presence of shock waves introduce complications in the modelling of the flow transition between the

static and rotating regions of the microturbine. All the simulation issues, options and model settings used are also described in [14].

2.1 Various seal designs

A simplified model of the microturbine stage was created. Five design modifications of the rotor seal were prepared. It is known that the design of the labyrinth seal can affect the parameters of turbomachines [14] such as efficiency and forces.

The model without seals was represented by the basic design (a). The most complicated seal design was the staggered labyrinth seal with six teeth (b). The simplified design was the see-through labyrinth with three teeth (c). The last design prepared in two variants was the staggered labyrinth seal with only one tooth – the first one located at the smaller diameter of the rotor (d) and the second one located at the larger diameter (e). All design variants are shown in Fig. 2.

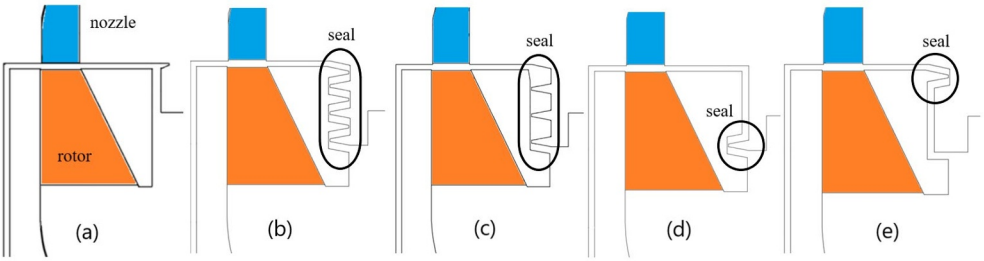

Fig. 2. Design of the seals geometry variants.

2.2 CFD model

NUMECA FINE/Turbo 11 [15] software was used to prepare, compute and evaluate the cases. The CFD model consists of the following parts/domains: microturbine stage (stator, rotor, outlet), labyrinth seals (leakage) and dead space between rotational and static parts. The stator consists of 12 nozzles and non-axisymmetric channels. The rotor consists of 30 blades. The geometry of the model is shown in Fig. 3.

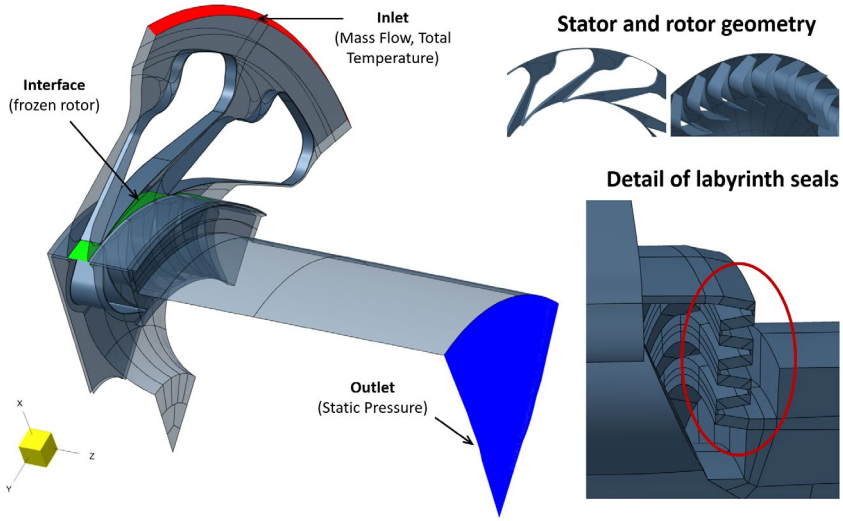

Fig. 3. CFD model of the micro-turbine stage – boundary conditions and geometry details.

The grid was created in NUMECA AutoGrid5 software. The mesh was hexahedral and multi-block structured with about 35 million cells. The mesh resolution had been studied and evaluated in previous simulations and it is sufficiently fine for our CFD model. The first cell at the wall is 0.0003 mm high and the maximum y^+ value in computations was 6.83.

A more complex EARSM turbulence model was used because the simulation results gained by using this model for complex geometries and complex flow structures are better with the NUMECA package than the results gained with the more commonly used Spalart – Almaras or SST k-ω models in "engineering" cases.

The working medium was set as the condensable gas model of hexamethyldisiloxane (MM). Properties of the fluid based on the NIST-REFPROP [16] are defined by tables generated in the NUMECA TabGen.

Boundary conditions were set as follows: at the inlet the variations of the total pressure p_{t0} and the total temperature T_{t0} at the outlet the area weighted average of the static pressure p_{s2} – see Table 1. The shaft revolution speed varied from 22.000 to 29.000 rpm. All walls were considered adiabatic. Steady solution was assumed.

Table 1. Inlet and outlet boundary conditions.

Revolutions [1/min]	Inlet total pressure [Pa]	Inlet total temperature [K]	Outlet pressure [Pa]
22,000	613,104	455.33	25,700
23,000	613,870	455.48	25,449
24,000	614,082	455.73	25,639
25,000	614,538	456.05	25,830
26,000	615,416	456.35	25,400
27,000	614,998	456.57	25,800
28,000	615,445	456.82	26,200
29,000	615,560	457.04	26,500

2.3 Evaluation

The planes and areas used for the evaluation of results are depicted in Fig. 4. The results were averaged during the last 1.500 iterations to obtain mean values for the evaluation.

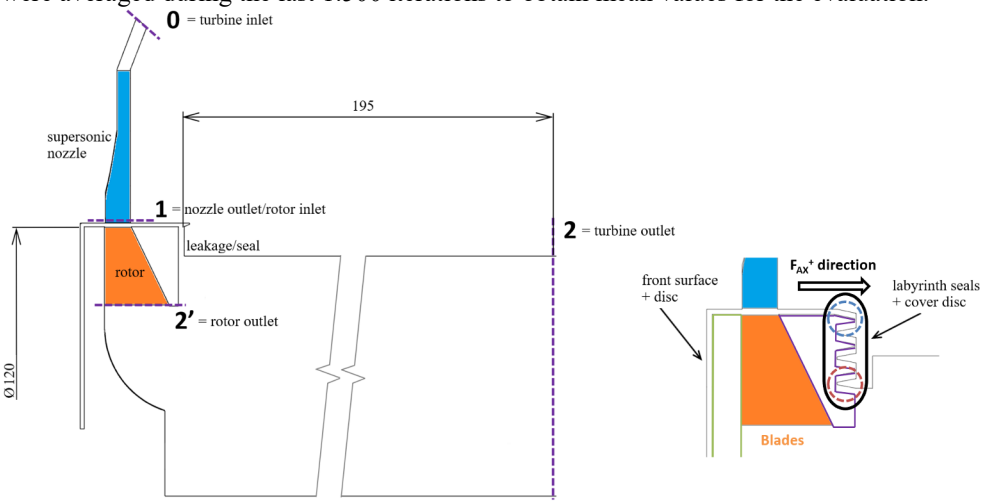

Fig. 4. Definition of evaluation planes and the areas for friction torque evaluation.

A very important value for turbomachines is efficiency. The total-to-static turbine efficiency (1) was evaluated from the computed torque M_T, the rotational speed n, the mass flow rate $\dot{m}$, the inlet total enthalpy h_{0T} and the outlet static enthalpy h_{2Sis} (which is a function of the inlet total entropy s_0 and the outlet static pressure p_{S2}).

$$\eta_{TS} = \frac{M_T \cdot 2 \cdot \pi \cdot n}{\dot{m} \cdot (h_{0T} - h_{2Sis})}, \tag{1}$$

where $$h_{2Sis} = f(s_0, p_{S2}).$$

3 Results

Numerical simulations were performed for all points of the working characteristic of the basic design (a) and for the staggered labyrinth seal with six teeth (b). The simulations were relatively time-consuming so the other design variants (c), (d) and (e) were simulated only for three speed values. This approach proved sufficient to obtain the results of these variants.

3.1 Efficiency

Table 2 shows the total-to-static turbine efficiency η_{TS} and the pressure ratio $\Pi = p_{t0}/p_{s2}$. The difference in the efficiency from 2 % to 4 % between the measurement and the simulations has already been discussed in [13]. It may be caused by the inaccuracy of the outlet pressure measurement and also by local inaccuracies on the rotor-stator interface. But the shapes of the characteristics are similar in all cases and it is possible to use CFD simulations to investigate the influence of various geometry changes on the turbine parameters.

Fig. 5 also shows that the efficiency of the designs with labyrinth seals is very similar to the basic design with only small differences.

Table 2. The total-to-static turbine efficiencies and the pressure ratios, experimental data from [4].

Revolutions [1/min]	η_{TS} [%]	Π [-]	η_{TS} [%]	Π [-]	η_{TS} [%]	Π [-]
	Experiment bas. des.		Basic design (a)		Labyrinth 6 teeth (b)	
22,000	69.37	23.87	71.77	23.87	71.97	23.87
23,000	71.30	24.12	73.59	24.13	73.75	24.13
24,000	73.36	23.96	75.18	23.96	75.55	23.97
25,000	74.29	23.81	76.55	23.81	77.17	23.81
26,000	75.32	24.23	77.72	24.24	77.81	24.24
27,000	75.80	23.85	78.84	23.87	78.87	23.87
28,000	76.09	23.52	79.52	23.54	79.37	23.54
29,000	74.71	23.27	79.80	23.26	79.16	23.27
	Labyrinth 3 teeth (c)		Labyrinth 1 s. t. d. (d)		Labyrinth 1 l. t. d. (e)	
22,000	72.13	23.87	72.09	23.87	72.16	23.87
25,000	76.83	23.81	76.79	23.81	76.77	23.81
28,000	79.40	23.54	79.44	23.54	79.46	23.54

Only a small increase in the efficiency can be observed at lower speeds, which gradually disappears. At the maximum revolution speed the effect is even rather negative – this effect is relatively surprising because better sealing should lead to the higher efficiency of the turbomachine.

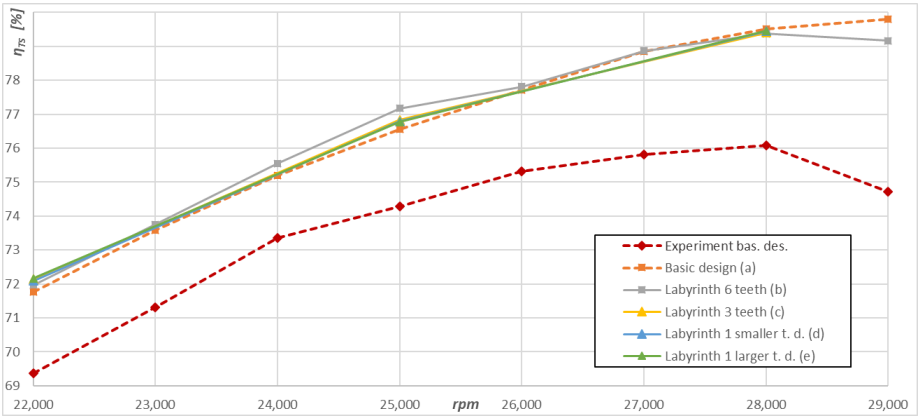

Fig. 5. The total-to-static turbine efficiencies, experimental data from [4].

3.2 Mass-flow rate

The computed total turbine mass-flow rate was about 0.33 kg/s for all cases and the rates were almost constant due to the choked flow in the supersonic stator nozzle. The value was about 2.8 % higher than the measured values. This is probably caused by the ideal geometry used in the CFD model.

Figure 6 shows the leakage mass-flow rate for the computed design geometries. The leakage mass-flow rate rises with the shaft revolutions and the values are significantly higher in the basic design than in the newly designed geometries with labyrinth seals. With the best sealing (b) the leakage mass-flow rate is only half that of the basic design. However, this positive and expected result has only a minimal impact on the predicted efficiency as is shown above. The benefit from reduced leakage flow is countered by the higher friction torque from the increased wetted area of the complex sealing geometries as shown below.

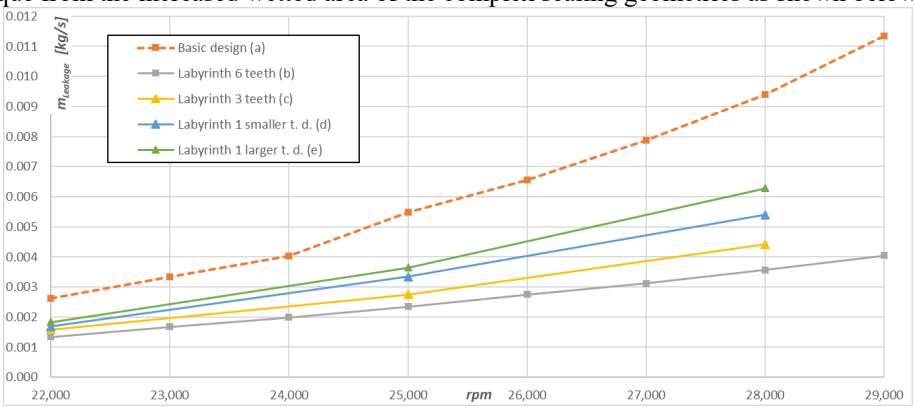

Fig. 6. The leakage mass flow rate.

3.3 Torque

The results mentioned above in 3.1 and 3.2 are followed by the analysis of the rotor torques. The total torque T_t decreases from about 6.8 Nm (22,000 rpm) to 5.6 Nm (29,000

rpm). This torque can be divided into individual components – the blade torque T_{blades} and the loss friction torques T_{front} (front surfaces/disc) and T_{seals} (seals/cover disc) according to relation (2). The calculated torque values can be found in Table 3. The T_{front} component has an almost constant T_{front} value around -0.026 Nm in all cases.

$$T_t = T_{blades} + T_{front} + T_{seals}. \quad (2)$$

Table 3. Evaluation of torque values.

Revolutions [1/min]	T_{blades} [Nm]	T_{seals} [Nm]	T_t [Nm]	T_{blades} [Nm]	T_{seals} [Nm]	T_t [Nm]
	Basic design (a)			**Labyrinth 6 teeth (b)**		
22,000	6.708	-0.004	6.679	6.744	-0.021	6.697
23,000	6.607	-0.003	6.579	6.641	-0.021	6.594
24,000	6.463	-0.003	6.434	6.513	-0.021	6.466
25,000	6.313	-0.001	6.286	6.374	-0.021	6.337
26,000	6.203	0.001	6.178	6.234	-0.023	6.185
27,000	6.032	0.003	6.009	6.06	-0.024	6.010
28,000	5.850	0.003	5.827	5.869	-0.025	5.817
29,000	5.647	0.004	5.624	5.632	-0.025	5.580
	Labyrinth 1 s. t. d. (d)			**Labyrinth 1 l. t. d. (e)**		
22,000	6.756	-0.018	6.708	6.76	-0.017	6.715
25,000	6.344	-0.014	6.306	6.343	-0.013	6.304
28,000	5.861	-0.013	5.821	5.86	-0.011	5.823

The value of the T_{seals} is very low in the basic design (a). The values of torque for all the labyrinth seals show that the T_{blades} increases in cases with higher rotor flow rates. T_+ is lower than the frictional loss torque. T_{seals} increases on the labyrinth surfaces, T_- especially at higher speeds, see Figure 7.

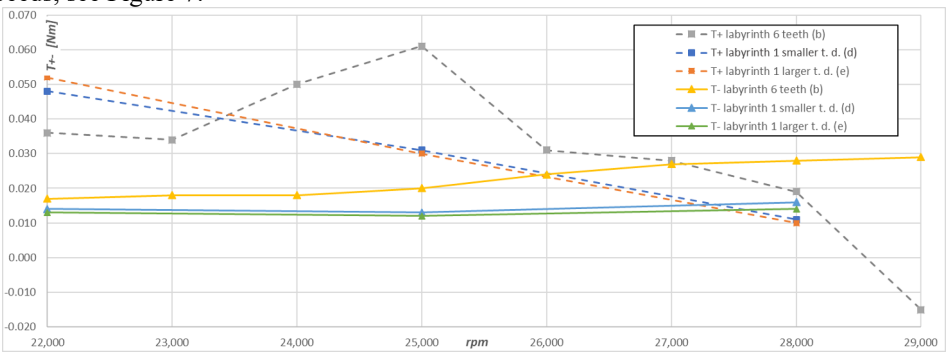

Fig. 7. The increase of the T_{blades} vs. the increase of the T_{seals}.

3.4 Axial force

The axial force value is important for the axial bearing design. The rotor axial force was evaluated and the values are shown in Fig. 8. The changing values for different seal designs can be seen.

While the forces are almost identical in the basic design (a) and the complex sealing (b), the use of one tooth and its position on the rotor (d) or (e) can partially influence the magnitude of the force. The position of the tooth influences the pressure distribution in the sealing channel. The smallest axial force was predicted for design (d) where the location of the seal is near the smaller diameter of the rotor.

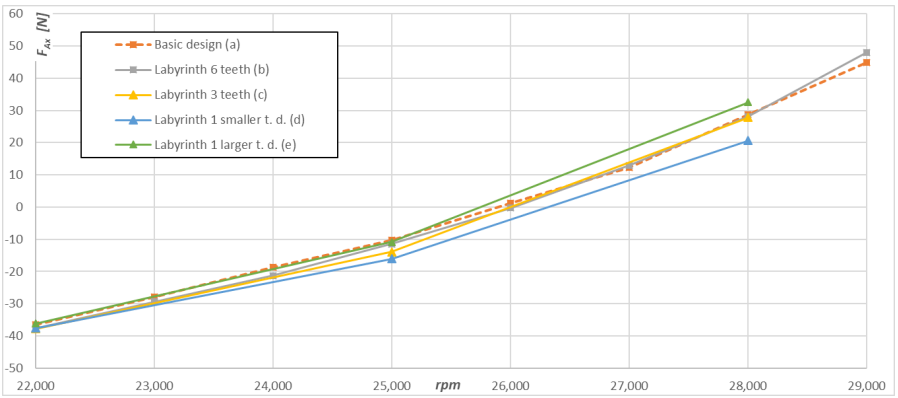

Fig. 8. The axial force acting on the rotor wheel.

3.5 Flow field

Fig. 9 shows the fields of the averaged velocity magnitude in ZR direction for 28,000 rpm for two designs. It shows that the presence of the labyrinth seal can influence the structure of the flow in the outlet part, but not significantly. The velocity fields in the other cases were similar to the labyrinth design with 6 teeth.

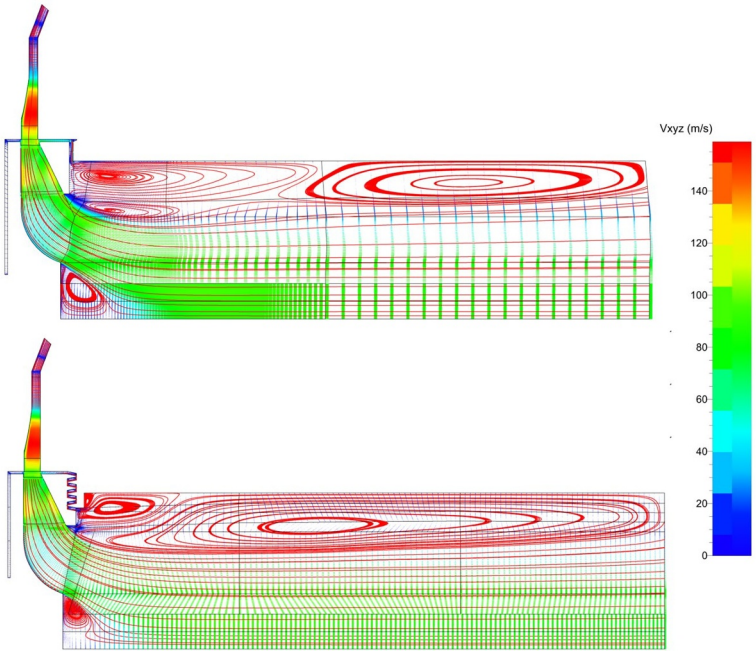

Fig. 9. Averaged velocity magnitude in ZR direction for 28,000 rpm, basic design (a) – top, labyrinth 6 teeth (b) – bottom.

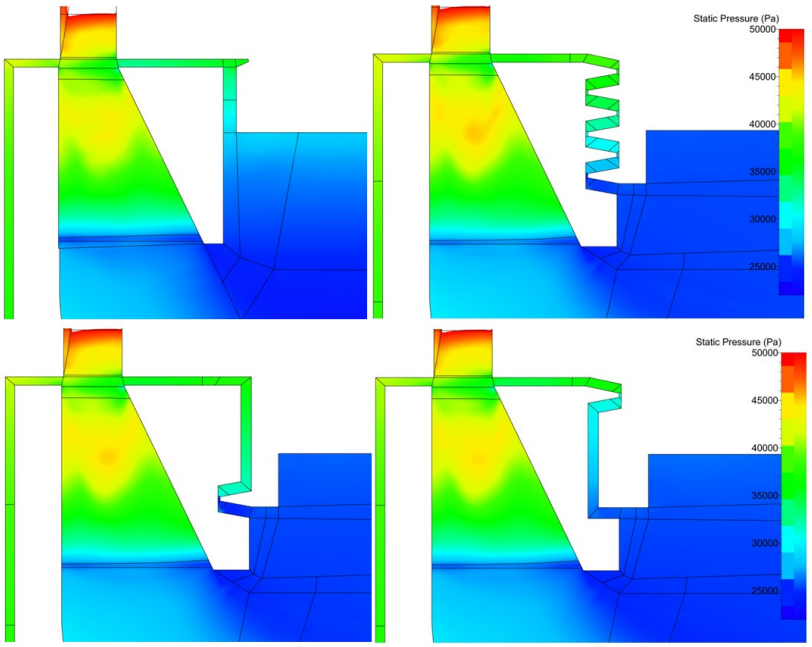

Fig. 10. Meridional averaged static pressure for 28 000 rpm, basic design (a) – top left, labyrinth 6 teeth (b) – top right, labyrinth 1 s. t. d. (d) – bottom left and labyrinth 1 l. t. d. (e) – bottom right.

The fields of the meridional averaged static pressure in Fig. 10 are more interesting. It is possible to see the changes in the pressure distribution in the turbine for various seal designs.

4 Discussion and conclusions

The numerical case study was carried out to determine the effect of the seals on the ORC micro-turbine parameters. Labyrinth seals used in the cantilever turbine design influence the working characteristics in several ways.

The leakage mass flow corresponds to the number of teeth used in the seals. The seal design (b) with six teeth reduces the mass flow to at least a half of the original value.

The most complicated staggered labyrinth seal with six teeth (b) has a positive effect on the turbine efficiency in the area of lower rotation speeds (about 0.3 %) but the effect is smaller than expected. The effect on the efficiency is zero in the area of the higher rotating speed (including the design point). The results of simulations thus showed that the increased friction eats up the gain in the blades. In the area of higher rotation speeds the influence of the friction on the larger surfaces negates the seal effect. All the efficiency values for the different labyrinth designs confirm this result, but it is necessary to consider the uncertainty of the results from the numerical solution for such complex flow fields.

Labyrinth seals with three or six teeth – (b), (c) have no practical effect on the axial force acting on the rotor wheel in comparison to the original geometry. This is due to the similar pressure distribution behind the rotor wheel. The labyrinth seals with one tooth (d) and (e) have an effect on the acting axial force in the order of ±6 N thus about 20 % higher or lower than the value of the basic design (a)) for 28,000 rpm. This effect is positive or negative depending on the tooth diameter.

The work has been supported by the project "Ziel - ETZ INTERREG V Project 53" and by the specific research – grant SGS-2022-023.

References

1. Cui, S., Zeng, P., Wang, Z, Zuo, Y. (2021). *Adaptive Current Protection Technology for Distribution Network with Distributed Power Sources Based on Local Information.* Mobile Information Systems, vol. 2021, Article ID 5137749. https://doi.org/10.1155/2021/5137749
2. Weiß, P. (2016). *Micro turbine generators for waste heat recovery and compressed air energy storage.* 15*th conference on Power System Engineering, Thermodynamics & Fluid Flows - ES2016*. Pilsen, Czech Republic.
3. Weiß, P. (2016). *Volumetric expander versus turbine – which is the better choice for small rc plants? 3rd International Seminar on ORC Systems* (22):301–310. http://www.asme-orc2015.be/content/publication.
4. Weiß, A.P., Popp, T., Müller, J., Hauer, J., Brüggemann, D. (2018). *Experimental characterization and comparison of an axial and a cantilever micro-turbine for small-scale Organic Rankine Cycle.* Appl Thermal Eng, 140 (2018), pp. 235-244 https://doi.org/10.1016/j.applthermaleng.2018.05.033
5. Fiaschi, D., Innocenti, G., Manfrida, G., Maraschiello, F. (2016). *Design of micro radial turboexpanders for ORC power cycles. From 0D to 3D.* Appl. Therm. Eng. ISSN 1359-4311 99 (2016) 402–410. https://doi.org/10.1016/j.applthermaleng.2015.11.087.
6. Da Silva, E.R., Kyprianidis, K.G., Camacho, R.G.R., Säterskog, M., Angulo, T.M.A. (2021). *Preliminary design, optimization and CFD analysis of an organic rankine cycle radial turbine rotor.* Appl. Therm. Eng. ISSN 1359-4311 195 (2021) 117103. https://doi.org/10.1016/j.applthermaleng.2021.117103.
7. Kaczmarczyk, T.Z., Żywica, G., Ihnatowicz, E. (2019). *Experimental study of a low-temperature micro-scale organic Rankine cycle system with the multi-stage radial-flow turbine for domestic applications.* Energy Convers Manage, 199 (2019), p. 111941, 10.1016/j.enconman.2019.111941
8. Weiß, A.P., Novotný, V., Popp, T., Streit, P., Špale, J., Zinn, G. et al. (2020). *Customized ORC micro turbo-expanders - From 1D design to modular construction kit and prospects of additive manufacturing.* Energy, 209 (2020), p. 118407, 10.1016/j.energy.2020.118407
9. Weiss, A.P., Streit, P., Popp, T., Shoemaker, P. (2020). *Uncommon turbine architectures for distributed power generation -development of a small velocity compounded radial re-entry turbine*. Archives of Thermodynamics, vol. 41, no. 4, pp. 235–253. DOI: 10.24425/ather.2020.135862
10. Weiß, A.P., Stümpfl, D., Streit, P., Shoemaker, P., Hildebrandt, T. (2022). *Numerical and Experimental Investigation of a Velocity Compounded Radial Re-Entry Turbine for Small-Scale Waste Heat Recovery.* Energies 2022, 15, 245. https://doi.org/10.3390/en15010245
11. Preißinger, M., Brüggemann, D. (2016). *Thermal stability of hexamethyldisiloxane (MM) for high-temperature organic rankine cycle (ORC).* Energies 9(183). Doi:10.3390/en9030183.
12. Preißinger, M., Schwöbel. J. (2017). *Multi-criteria evaluation of several million working fluids for waste heat recovery by means of organic Rankine cycle in passenger cars and heavy-duty trucks.* Applied Energy (206):887–899.

Doi:10.1016/j.apenergy.2017.08.212.

13. Turunen-Saaresti, T. (2017). *Design and testing of high temperature micro-orc test stand using siloxane as working fluid.* Journal of Physics: Conference Series (821). Doi:10.1088/1742-6596/821/1/012024.
14. Syka, T., Weiß, A. (2018). CFD flow analysis of the cantilever micro-turbine. *Acta Polytechnica CTU Proceedings 20:108–113.* Doi: 10.14311/APP.2018.20.0108
15. Wu, T., San Andrés, L. (2019). *Gas labyrinth seals: On the effect of clearance and operating conditions on wall friction factors – A CFD investigation*. Tribology International, Volume 131, 2019, 363-376. ISSN 0301-679X. https://doi.org/10.1016/j.triboint.2018.10.046.
16. NUMECA-Online, https://www.numeca.com/home (retrieved on 09.12.2019)
17. NIST-REFPROP, https://www.nist.gov/srd/refprop (retrieved on 09.12.2019)